

INFLUENCE OF COARSE AGGREGATE SHAPE ON THE STRENGTH OF ASPHALT CONCRETE MIXTURES

Jian-Shiuh CHEN
Professor
Department of Civil Engineering
National Cheng Kung University
1 University Road
Tainan 701, Taiwan
Fax: +886-6-235-8542
E-mail: jishchen@mail.ncku.edu.tw

M.K. CHANG
Ph.D. Candidate
Department of Civil Engineering
National Cheng Kung University
1 University Road
Tainan 701, Taiwan
Fax: +886-6-235-8542
E-mail: e899299@ms32.hinet.net

K.Y. LIN
Ph.D. Candidate
Department of Civil Engineering
National Cheng Kung University
1 University Road
Tainan 701, Taiwan
Fax: +886-6-235-8542
E-mail: cutesalmon@sinamail.com

Abstract: The objectives of this paper are to evaluate aggregate characteristics including elongation, flatness, and other shape indices. The following particle shapes were selected for this study: cubical, rod, disk, and blade. The change in rotation angle of coarse aggregate was found to correlate well with the internal resistance of a HMA mix. The particle index (*PI*) was shown to be an adequate measure of the combined contribution of particle shape, angularity, and surface texture to the stability of an aggregate. The *PI* value correlated well to aggregate geometric characteristics including elongation ratio, flatness ratio, shape factor, and sphericity. Cubical particles were desirable for increased aggregate internal friction and improved rutting resistance. The more cubical the aggregate, the higher the *PI* value. The *PI* value of coarse aggregate significantly affected the engineering properties of a HMA mix. The particle shape determined how aggregate was packed into a dense configuration and also determined the internal resistance of a mix. Of the four particle shapes evaluated, the cubical aggregate demonstrated the best rutting resistance. Flaky and/or elongated aggregate was shown to have lower compactibility and higher breakage.

Key Words: particle orientation, coarse aggregate, aggregate shape, hot mix asphalt

1. INTRODUCTION

Mineral aggregate constitutes approximately 95% of hot-mix asphalt (HMA) by weight. The mineral aggregate is made up predominantly of coarse aggregate. Research has shown that aggregate characteristics such as particle size, shape, and texture influence the performance and service ability of hot-mix asphalt pavement (Brown et al. 1989; Kandhal et al. 1992; Kim et al. 1992). Flat and elongated particles tend to break during mixing, compaction, and under traffic. Therefore, aggregate shape is one of the important properties that must be considered in the mix design of asphalt pavements to avoid premature pavement failure. The recent Strategic Highway Research Program (SHRP) targeted primarily asphalt binder properties and their contribution to pavement performance. Detailed investigations of aggregate contributions to pavement performance were excluded from the program. Furthermore, specifications in Taiwan have recommended changing the definition of flat and elongated

aggregate from a dimensional ratio of 3:1 to 5:1. Engineering justification data are required to establish rationally the criteria for this change.

Aggregate morphological characteristics are very complex and cannot be characterized adequately by any single test. As a result, conflicting results have been reported on how aggregate shape influences the quality of HMA mixtures. For example, Shklarsky and Livneh (1964) concluded that replacing uncrushed coarse aggregate with crushed coarse material did not significantly improve the asphalt mix properties. Krutz and Sebaaly (1993) found a direct correlation between the rutting potential of HMA mixtures and the shape and texture of coarse aggregate particles. Li and Kett (1967) concluded in their study that flat and elongated particles could be permitted in a mixture without adverse effect on its strength. Some mixes with flaky aggregates have been found to exhibit higher fatigue life than mixes with nonflaky aggregates. Oduroh et al. (2000) showed that the percentage of crushed coarse particles had a significant effect on laboratory permanent deformation properties. As the percentage of crushed coarse particles decreased, the rutting potential of the HMA mixtures increased. Huber and Heiman (1987) found that crushed aggregate containing 19% flat and elongated particles did not adversely affect the volumetric properties of HMA mixtures. Stephens and Sinha (1978) presented data on the effect of aggregate shape, and recommended blends of regular particles, flat particles, and rod-like particles to achieve optimum strength. Kalcheff and Tunnicliff (1982) discussed the effect of crushing, aggregate size, and particle shape. They emphasized that asphalt usage can be reduced by increasing the size of crushed aggregate used in a mix. These conflicting statements result primarily from the lack of better understanding of the effect of aggregate shape on engineering properties of a HMA mix.

Visual examination is the most common method of judging aggregate shape. Because of the tedious task of making numerous readings, the civil engineer generally finds it impractical to identify particle shape visually. Various innovative methods are available to facilitate the quantification for aggregate shape. One of the most effective methods is digital image processing and analysis. This method provides the capability of quick and accurate measurement of the characteristics of aggregate particles. For example, Yue et al. (1995) used a digital image processing technique to quantify the distribution, orientation, and shape of coarse aggregate. Their quantitative results indicated that microstructural characteristics of asphalt concrete mixtures could be measured accurately using a digital image processing technique. Kuo et al. (1998) also used three-dimensional image analysis techniques of aggregate particles to measure the shape, size, and diameter of the particles. Therefore, the objectives of this paper are (1) to quantify the morphological characteristics of coarse aggregate, (2) to evaluate the engineering properties of HMA mixtures made of different aggregate shapes, and (3) to characterize the aggregate orientation during traffic loading.

2. MATERIALS AND METHODS

2.1 Aggregate

Crushed limestone was employed to produce two aggregate gradations, given in Table 1. These two gradations (i.e., open and dense) represent two examples of the influence of aggregate shape. The stone-mastic asphalt (SMA) mixture is an open gradation that provides a strong aggregate structure using coarse particles. The dense gradation is a typical gradation used by highway agencies in Taiwan, and the aggregate structure is supported by continuous particle sizes. Coarse and fine aggregate refers to materials retained on and passing through

the 4.75-mm sieve, respectively. The coarse aggregate was sieved and partitioned into four size fractions, namely, 25 to 19 mm, 19 to 12.5 mm, 12.5 to 9.5 mm, and 9.5 to 4.75 mm (3/4 to 1/2 in., 1/2 to 3/8 in., and 3/8 in. to #4). The fine aggregate was sieved and partitioned into seven size fractions as in Table 1.

Table 1. Physical Properties and Aggregate Gradations

Type	Specific gravity	L.A. Abras. (%)	Size distribution (% passing by weight)										
			25 mm	19 mm	12.5 mm	9.5 mm	4.75 mm	2.36 mm	1.18 mm	0.6 mm	0.3 mm	0.15 mm	0.075 mm
SMA	2.64	20.5	100	91.2	46.3	38.2	23.7	19.9	17.6	15.9	14.3	12.3	9.6
Dense	2.64	20.5	100	90	80	70	57	43	-	25	18	11	4

The coarse size fractions of SMA were evaluated for the influence of aggregate shape on engineering properties of a HMA mix. Aggregate shape analysis was carried out through the use of the Zingg diagram on the basis of the particle longest diameter (d_L), the intermediate diameter (d_I), and the shortest diameter (d_S) (1935). The selection process was carefully conducted by an image analyzer, as discussed in the next section. The elongation ratio and the flatness ratio were used to define the aggregate shape as shown in Figure 1. The former is the ratio of d_I to d_L , and the latter is the ratio of d_S to d_I . Four different aggregate shapes were selected as follows: disk, blade, rod, and cube. As both ratios are equal to or larger than 2/3, the cubical aggregate was selected for the HMA mix in order to contrast it with the mixes consisting of other shapes. The disk-shaped aggregate is flaky and oblate, the rod-shaped is elongated, and the blade-shaped is both flaky and elongated.

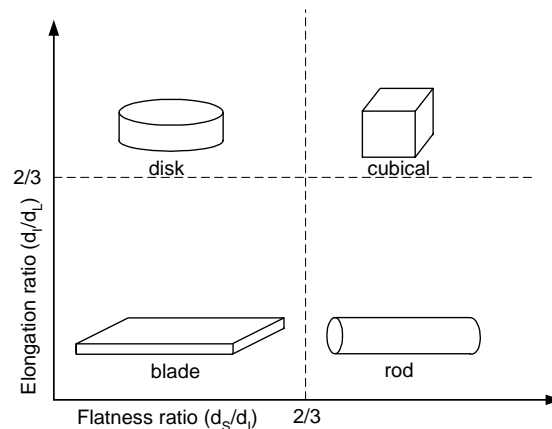


Figure 1. Aggregate Shapes Used in This Study

2.2 Image Measurements of Coarse Aggregate

Image analysis techniques were used in this study to characterize the morphological characteristics of coarse aggregate particles. The system consists of two major assemblies – a microscope with a scanner, and a rack of modules – basic, display, control, and measurement. The device, called Optimas image analyzer, is versatile software capable of providing full measurements of coarse aggregate.

Aggregate particles were attached to adhesive clear plastic trays with two perpendicular faces; then, the sample tray was rotated 90° to establish two orthogonal planes of measurement.

Particles were placed on a light box that illuminated the sample and made definite contact between aggregate and background. The parameters of length, width, and thickness were obtained by measuring the two orthogonal planes. These parameters provided a direct method for determining the flatness and the elongation ratios of the particles. Additionally, the image analysis method provided other shape indices that could be related to the effects of aggregates on the properties of a HMA mix. This image analysis method was more time-efficient than the ASTM Test Method for Flat Particles, Elongated Particles, or Flat and Elongated Particles in Coarse Aggregate (D 4791). The imaging processing technique also provided more information.

2.3 Particle Index of Coarse Aggregate

The combined effects of particle shape and surface texture of an aggregate were determined in accordance with ASTM Test Method for Index of Aggregate Particle Shape and Texture (D 3398). The equipment required for this test consists basically of a cylindrical steel mold 152 mm (6 in.) in diameter by 178 mm (7 in.) high, and a steel rod 16 mm (5/8 in.) in diameter by 610 mm (24 in.) long with the tamping end rounded to a hemispherical tip. A clean, washed, oven-dried, single-size aggregate fraction was used for this test. The mold was filled in three equal layers, with each layer compacted with 10 well-distributed blows of the tamping rod. Each tamp consisted of a drop with the tamping rod from 51 mm (2 in.) above the surface of the layer being compacted. This procedure was repeated using the same material but applying 50 blows on each of the three layers. The weight of the contents of the mold in each case was determined and the corresponding percentage of voids was calculated using the bulk specific gravity of each aggregate fraction. The particle index (*PI*) is derived using the following equation:

$$PI = 1.25V_{10} - 0.25V_{50} - 32 \quad (1)$$

where

V_{10} = percent voids in the aggregate compacted with 10 blows per layer;

V_{50} = percent voids in the aggregate compacted with 50 blows per layer.

2.4 Mixture Design

Mixture designs were performed using the Marshall method by preparing and compacting samples with asphalt content varied in 0.5% increments according to ASTM Test Method for Resistance to Plastic Flow of Bituminous Mixtures Using Marshall Apparatus (D 1559). Grade AC-20 asphalt binder from the Chinese Petroleum Corporation was used in this study. Specimens were compacted with 50 blows on each side. Three samples were made for each asphalt content. Approximately 0.3% cellulose fiber was added to the SMA mixture to prevent draining down. The optimum asphalt content was chosen as the asphalt content that produced 4% air voids. Further, two types of void were calculated for the compacted samples: the void in mineral aggregate (*VMA*), and the void space in coarse aggregate (*VCA*). The *VCA*'s were calculated in a way similar to the *VMA*'s by replacing percent of aggregate in the mix with percent of coarse aggregate in the calculation. The equations used for calculating *VMA* and *VCA* are as follows:

$$VMA = 1 - \frac{V_{agg}}{V_T} \quad (2)$$

$$VCA = 1 - \frac{V_{ca}}{V_T} \quad (3)$$

where

- V_{agg} = volume of aggregate,
- V_T = total volume of compacted mixture,
- V_{ca} = volume of coarse aggregate

2.5 Indirect Tension Test

The resilient modulus and the indirect tensile strength of HMA are used often to evaluate the relative quality of materials. The repeated-load indirect tension test for determining the resilient modulus was conducted by applying compressive loads with a haversine waveform according to ASTM Test Method for Indirect Tension Test for Resilient Modulus of Bituminous Mixtures (D 4123). The load was applied vertically in the vertical diameter plane of a cylindrical specimen of asphalt concrete through a curved loading strip. The resulting horizontal deformation was measured and used to calculate the total resilient modulus (M_r) as follows:

$$M_r = \frac{P \cdot (v + 0.27)}{t \cdot H} \quad (4)$$

where

- P = repeated load,
- v = Poisson's ratio,
- t = thickness of specimen,
- H = total recoverable horizontal deformation.

Poisson's ratio was calculated using the measured recoverable vertical and horizontal deformation. The tensile strength (S_T) is calculated as follows:

$$S_T = \frac{1.96 \cdot P_{ult}}{\pi \cdot t \cdot D} \quad (5)$$

where

- P_{ult} = ultimate applied load required to cause to the specimen to fail,
- t = thickness of specimen,
- D = diameter of specimen.

2.6 Wheel-tracking Test

A wheel-tracking test was performed to evaluate the susceptibility of a mixture to permanent deformation. This equipment is similar to the Hamburg Wheel-Tracking Device. Mixture samples of different binders were carefully controlled to have the same binder content, air void content, gradation, and aggregate type. The test was conducted at the mean highest weekly average temperature, which was set at temperature 60°C under dry conditions. A smooth solid-steel wheel traveling at a speed of 1.4 km/h was used to correlate with rutting. Rut depths were measured every 200 wheel passes on 300 mm x 300 mm x 70 mm samples.

3. RESULTS AND DISCUSSION

3.1 Particle Shape Analysis

Particle shape analysis was carried out in terms of elongation ratio, flatness ratio, shape factor, and sphericity using an image analyzer. The mean value for each aggregate size is listed in Table 2. The results show that there exist distinct morphological characteristics for different particle shapes. The differentiation of different aggregate shapes agrees well with the definition in Figure 1 according to flatness and elongation ratios. For cubical particles, the flatness ratio is 0.80 and elongation 0.81, and both values are larger than $2/3$. Note that, in cubical limestone, particles in the size range 25 to 19 mm are the most spherical, and those in the size range 9.5 to 4.75 mm are relatively flat and elongated. The dense gradation appears to be the combination of four different shapes since both ratios approach $2/3$. Data in Table 2 indicate that the higher the shape factor, the more nearly cubical the aggregate. For aggregate used in pavement construction, the shape factor is generally between 0.3 and 0.8. Aggregate used in this study falls within this range. The sphericity value represents the roundness of an aggregate regardless of its thickness. Cubical particles possess a higher sphericity value than do the others. The typical sphericity value is between 0.5 and 0.9, which corresponds well with the description of each aggregate shape.

3.2 Particle Index (PI)

The particle index of an aggregate containing several sizes is weighted on the basis of the percentage of the fractions in the original grading of the aggregate. Table 3 lists the procedure to calculate the *PI* value for each aggregate shape. The weighted value is the product of the aggregate grading times the corresponding particle index of each size group. The *PI* is the summation of the weighted values, which are 17.0, 15.8, 14.8, 12.7, and 15.2 for cubical, rod, disk, blade, and dense aggregate, respectively. A higher *PI* value implies that the particle shape is closer to cubical. The flat and elongated aggregate is associated with a lower *PI*. For the dense gradation conventionally used, the *PI* value is 15.2, which agrees well with values reported by other researchers (Boutilier 1967; Huang 1970; Livneh, Greenstein 1972; McLeod, Davidson 1981).

Four aggregate characteristics (elongation ratio, flatness ratio, shape factor, and sphericity) in Table 2 were correlated with the particle index. The relationship between predicted *PI* and measured *PI* is shown in Figure 2. Aggregate composed of flat and elongated particles may have a low particle index of 10 or less, while aggregate consisting of highly cubical particles can have a particle index of 18 or more. The coefficient of determination (R^2) is 0.85, indicating that there exists a strong correlation between measured *PI* and the *PI* calculated using the aggregate geometric characteristics.

Table 2. Aggregate Geometric Characteristics from Image Analysis

Shape	Size (mm)	d_L (mm)	d_l (mm)	d_s (mm)	Elong. ¹	Flat. ²	Shape ³	Spher. ⁴
Cubical	25-19	23.25	19.75	17.32	0.85	0.88	0.81	0.86
	19-12.5	18.32	15.02	11.28	0.82	0.78	0.68	0.80
	12.7-9.5	14.05	11.34	9.08	0.81	0.80	0.72	0.80
	9.5-4.75	9.58	7.39	5.74	0.77	0.75	0.68	0.77
Avg.					0.81	0.80	0.72	0.81
Rod	25-19	29.89	16.58	14.85	0.55	0.90	0.67	0.65
	19-12.5	26.58	14.75	11.88	0.55	0.81	0.60	0.63
	12.7-9.5	18.69	10.89	8.88	0.58	0.82	0.62	0.65
	9.5-4.75	13.85	9.057	7.18	0.65	0.79	0.64	0.70
Avg.					0.59	0.83	0.63	0.66
Disk	25-19	24.78	23.45	13.85	0.95	0.59	0.57	0.81
	19-12.5	20.87	17.98	10.32	0.86	0.57	0.53	0.75
	12.7-9.5	15.36	13.02	8.01	0.85	0.62	0.57	0.76
	9.5-4.75	11.01	8.98	5.32	0.82	0.59	0.54	0.73
Avg.					0.87	0.59	0.55	0.76
Blade	25-19	37.12	22.87	14.32	0.62	0.63	0.49	0.62
	19-12.5	29.31	17.38	11.32	0.59	0.65	0.50	0.61
	12.7-9.5	20.96	12.87	5.38	0.61	0.42	0.33	0.54
	9.5-4.75	15.85	7.98	3.25	0.50	0.41	0.29	0.47
Avg.					0.58	0.53	0.40	0.56
Dense	25-19	30.52	22.32	13.85	0.73	0.62	0.55	0.68
	19-12.5	27.54	17.25	10.58	0.63	0.61	0.47	0.59
	12.7-9.5	18.32	11.22	5.85	0.61	0.52	0.39	0.54
	9.5-4.75	10.36	6.25	4.85	0.60	0.78	0.55	0.58
Avg.					0.64	0.63	0.49	0.60

1: Elongation ratio = d_l / d_L

2: Flatness ratio = d_s / d_l

3: Shape factor = $d_s / \sqrt{d_l \cdot d_L}$

4: Sphericity = $\sqrt[3]{d_s \cdot d_l / d_L^2}$

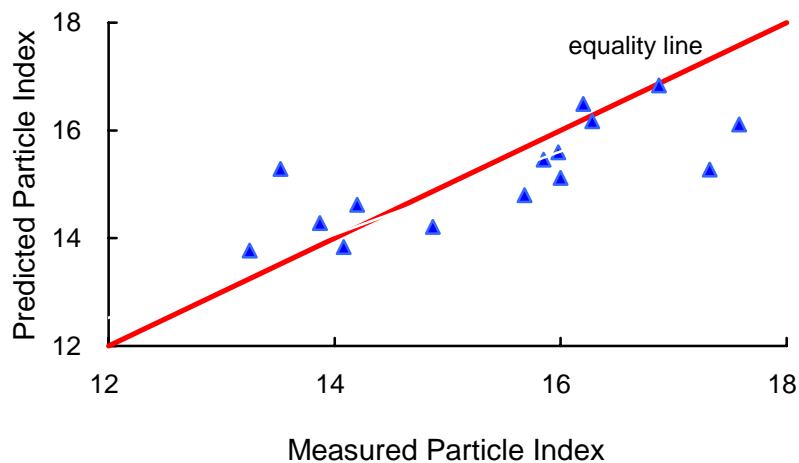


Figure 2. Relationship Between Measured *PI* and Predicted *PI*

Table 3. Measured Particle Index (*PI*) for Coarse Aggregate

Shape	Size (mm)	Retained (%)	<i>PI</i> for each size	Weighted value
Cubical	25-19	11.5	18.6	2.1
	19-12.5	58.8	17.6	10.3
	12.7-9.5	10.6	15.7	1.7
	9.5-4.75	19.0	15.2	2.9
<i>PI</i>				17.0
Rod	25-19	11.5	17.1	2.0
	19-12.5	58.8	16.3	9.6
	12.7-9.5	10.6	14.9	1.6
	9.5-4.75	19.0	14.0	2.7
<i>PI</i>				15.8
Disk	25-19	11.5	16.9	1.9
	19-12.5	58.8	15.1	8.9
	12.7-9.5	10.6	14.1	1.5
	9.5-4.75	19.0	13.3	2.5
<i>PI</i>				14.8
Blade	25-19	11.5	15.2	1.8
	19-12.5	58.8	12.8	7.5
	12.7-9.5	10.6	12.3	1.3
	9.5-4.75	19.0	11.2	2.1
<i>PI</i>				12.7
Dense	25-19	23.3	17.3	4.0
	19-12.5	23.3	15.7	3.6
	12.7-9.5	23.3	14.9	3.5
	9.5-4.75	30.2	13.5	4.1
<i>PI</i>				15.2

3.3 Marshall Design Values

The Marshall test is a routine test that enables one to determine strength indexes such as stability and flow for the design of a HMA mixture. Other mixture design criteria such as asphalt content and air void content are also obtained from this test. Table 4 lists the mixture characteristics of different aggregate shapes. Statistical analysis with $\alpha = 0.05$ for flow and asphalt content shows no statistically significant differences among the mixes in Table 4. These results give an indication that these properties of the mixes made of different particle shapes are equal. A p -value less than 0.05, however, indicates statistical significance in which the aggregate shape affects the behavior of a HMA mix. HMA mixtures containing flaky aggregate have a significantly higher void percentage than similar mixtures containing cubical aggregate. Flaky particles produce a lower Marshall stability. This implies that blade and disk aggregates have low compatibility, thus contributing to lower stability values.

Table 4. Marshal Mix Design Properties

	Blade	Disk	Rod	Cubical	Dense	p -value
Stability (kN)	7.2	7.8	9.6	10.7	8.3	0.013
Flow (0.25 mm)	15	15	14	13	15	0.530
Asphalt content (%)	6.2	6.3	6.2	6.3	5.5	0.195
VMA (%)	18.8	18.5	17.8	17.2	13.3	0.031
VCA (%)	16.4	16.2	15.8	15.4	12.5	0.025

3.4 Indirect Tensile Test and Resilient Modulus

Conventionally, the indirect tensile test and resilient modulus test are conducted to indicate the internal resistance in a mix. Mixes were prepared to observe the effect of aggregate shape on the strength of the mixes. Figure 3 shows the test results for different aggregate shapes with PI values in the parenthesis. The resilient modulus is observed to increase with increasing PI value. A similar trend was also observed for indirect tensile strength. Coarse aggregate with lower PI provides lower stiffness than one with higher PI . Blade and disk particles impede compaction and thus may prevent the development of satisfactory properties in HMA. In compacted mixtures, cubical particles exhibit interlock and internal friction, and hence result in greater mechanical stability than do flat, thin, and/or elongated particles. The PI value is a quantitative measure of the aggregate shape that influences the characteristics of HMA mixtures. Test method ASTM D 3398 provides an adequate index to indicate the effects of the aggregate shape on the engineering properties of a HMA mix.

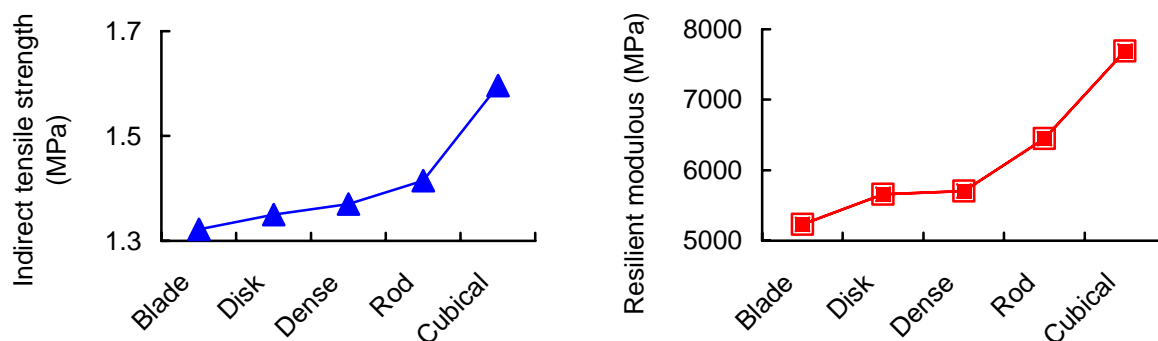


Figure 3 Effect of Aggregate Shape on Indirect Tensile Strength and Resilient Modulus

3.5 Rutting Resistance

Figure 4 shows the results obtained from the wheel-tracking test for different aggregate shapes. Mixtures with cubical aggregate clearly show better rutting resistance than do the others. As aggregate shape becomes cubical, the internal resistance appears to initiate at an early stage, i.e., around 300 s after loading. When cubical coarse aggregates make contact, stone-on-stone interlocking inside the HMA mix takes place. Conversely, the skeleton of elongated and/or flaky aggregate remains relatively unstable. Note that flat and elongated particles are more difficult to compact, and may result in a weak aggregate structure.

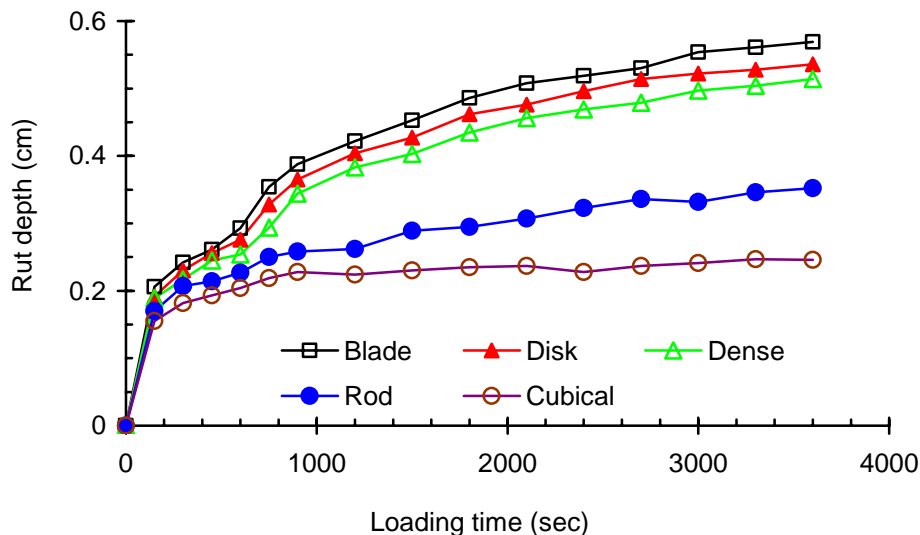


Figure 4. Rut Depth Versus Loading Time

Stone-on-stone contact for the blade aggregate is shown to begin at much later time. The results shown in Figure 4 validate the internal resistance as discussed in Figure 3. As the shape of coarse aggregate changes to be more cubical, the internal resistance increases and the HMA mix improves its capability of carrying traffic load. The cubical particles possess the highest rutting resistance, following by rod, dense, disk, and blade particles. It appears that a HMA mix can be made more stable and resistant to rutting by specifying the coarse aggregate shape, i.e., by specifying the flatness ratio, the elongation ratio, and the aggregate angularity.

Samples after the wheel-tracking test were studied to determine if their gradations changed with the application of traffic loading. Figure 5 shows a higher breaking percentage in HMA mixes containing the blade aggregate than the cubical aggregate. This breakage favors the formation of voids free of asphalt binder and fines, which causes the specimen to weaken. It is shown in Figure 5 that blade particles increase the breakage percentages between sieve sizes 12.5 mm and 4.75 mm (#4 sieve). Flat particles, thin particles, or long, needle-shaped particles break more easily than do cubical particles. The degradation of flaky aggregate also leads to poorer mechanical properties.

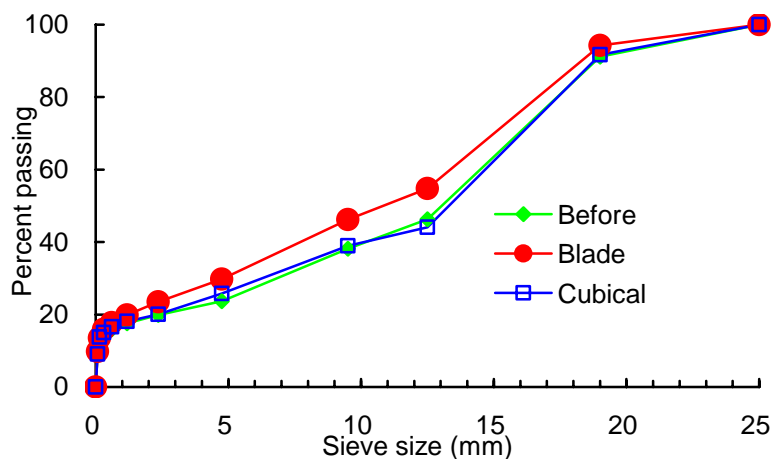


Figure 5. Aggregate Gradations Before and After Wheel-Tracking Test

3.6 Aggregate Orientation

Utilizing the image processing technique makes it possible to observe the internal resistance in a HMA mix during the wheel-tracking test. A cross-section is cut and the rotation change of coarse aggregates examined after loading is applied. Images of cross sections are taken and analyzed before and after testing. Figure 6 shows the aggregate cross-sections before and after the wheel-tracking test.

The rest angle is measured to examine how the internal resistance develops in a mix. The angle between the long axis of a coarse aggregate particle and the horizontal line is defined as the rest angle. Figs. 7 and 8 illustrate the change in rest angle before and after the wheel-tracking test for cubical and blade aggregates, respectively. The rest angle is divided into three groups: 0° to 30° , 31° to 60° , and 61° to 90° , representing the degree of coarse aggregates settling down in a mix. A higher portion of 0° to 30° rest angles indicates a stable mix in which internal resistance is ready to mobilize once external loading is applied, whereas the 61° to 90° range is a sign of an unstable condition. The intermediate range of 31° to 60° is a transition area either from unstable to stable conditions or visa versa.



(a) Before wheel-tracking test



(b) After wheel-tracking test

Figure 6. Image of Cross-Section for Mixture

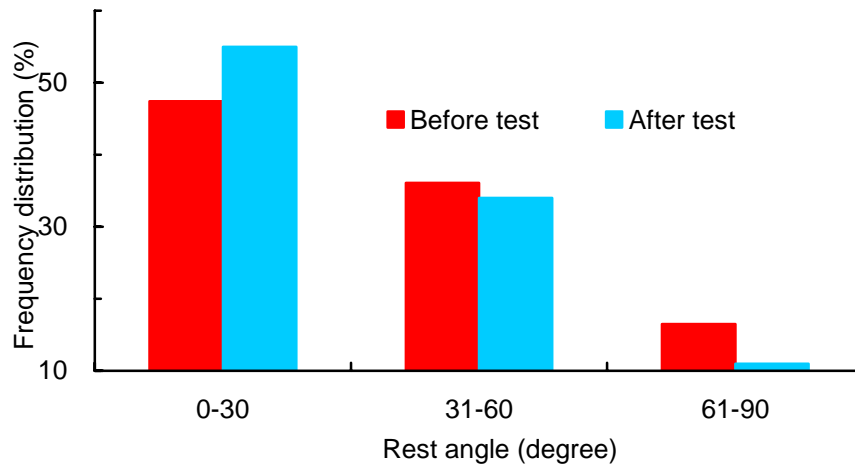


Figure 7. Rest Angle Distribution for Cubical Aggregate

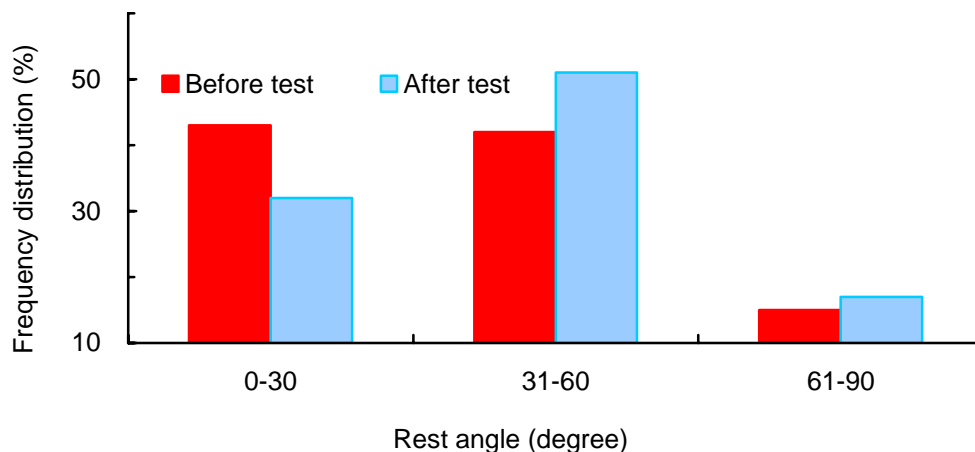


Figure 8. Rest Angle Distribution for Blade Aggregate

Mixtures with cubical particles show more stable rest angles (0° to 30°) than do blade ones. Especially after the test, the former mix becomes more stable with more than 55% of coarse aggregates settling within the 0° to 30° range, whereas the latter one results in the reduction of stable rest angles. Figure 7 shows that the cubical particles are in greater contact with each other, a sign of developing internal resistance to rutting. The transition range 31° - 60° significantly increases for mixtures with blade particles. The decrease in 0° to 30° and the increase in 31° to 60° rest angles may lead to an unstable skeleton inside mixtures with blade particles. Image evaluation of aggregate rotation is in good agreement with previous results on the determination of internal resistance.

4. CONCLUSIONS

Four different shapes of aggregate were evaluated to determine the engineering properties of hot-mix asphalt mixtures. The resilient modulus and the indirect tensile strength of HMA were used to evaluate the relative quality of materials. A wheel-tracking test was also performed to evaluate the susceptibility of a mixture to permanent deformation. The image analyzer was shown to be a useful tool for quantifying the morphological characteristics of coarse aggregate. Image evaluation provided quantitative indices such as geometric measurement and angle rotation of granular materials. Data showed that the morphological characteristics of coarse aggregate correlated well with the results of other indirect tests such as the particle index. Cubical particles possessed the best rutting resistance over the other shapes. Flaky and/or elongated aggregate in a mixture resulted in a lower resistance to shear deformation. The particle index (*PI*) was shown to be an adequate measure of the combined contribution of particle shape, angularity, and surface texture to the stability of an aggregate. The *PI* value correlated well to aggregate geometric characteristics including elongation ratio, flatness ratio, shape factor, and sphericity. The particle shape determined how aggregate was packed into a dense configuration and also determined the internal resistance of a mix. Of the four particle shapes evaluated, the cubical aggregate demonstrated the best rutting resistance. Flaky and/or elongated aggregate was shown to have lower compactibility and higher breakage. The morphological characteristics of coarse aggregates found from image analysis were in good agreement with the engineering properties of hot-mix asphalt mixtures. This paper presents a precise method to evaluate the aggregate characteristics in a HMA mix and demonstrates their effects on pavement performance. The results of this paper would provide useful guidelines for highway engineers to construct a long-lasting pavement.

ACKNOWLEDGEMENTS

The authors are very grateful to the National Science Council (NSC92-2211-E-006-097) for sponsoring this study.

REFERENCES

- Boutilier, O.D. (1967) A study of the relation between the particle index of the aggregate and the properties of bituminous aggregate mixtures. **Proceedings of Association of Asphalt Paving Technologists**, 36, 157-179.
- Brown, E.R., McRae, J.L., and Crawley, A.B. (1989) Effect of aggregate on performance of bituminous concrete. **ASTM STP 1016**, Philadelphia, 34-63.
- Huang, E.Y. (1970) A study of strength characteristics of asphalt-aggregate mixtures as affected by the geometric characteristics and gradation of aggregate. **Proceedings of Association of Asphalt Paving Technologists**, 39, 98-133.
- Huber, G.A., and Heiman, G.H. (1987) Effect of asphalt concrete parameters on rutting performance: a field investigation. **Proceedings of Association of Asphalt Paving Technologists**, 56, 33-61.

Kalcheff, I.V., and Tunnicliff, D.G. (1982) Effects of crushed stone aggregate size and shape on properties of asphalt concrete. **Proceedings of Association of Asphalt Paving Technologists**, 51, 453-483.

Kandhal, P.S., Khatri, M.A., and Motter, J.B. (1992) Evaluation of particle shape and texture of mineral aggregates and their blends. **Journal of Association of Asphalt Paving Technologists**, 61, 217-240.

Kim, Y.R., Yim, N., and Khosla, N.P. (1992) Effect of aggregate type and gradation on fatigue and permanent deformation of asphalt concrete. **ASTM STP 1147**, Philadelphia, 310-328.

Krutz, N.C., and Sebaaly, P.E. (1993) Effect of aggregate gradation on permanent deformation of asphaltic concrete. **Proceedings of Association of Asphalt Paving Technologists**, 62, 450-473.

Kuo, C.Y., Rollings, R.S., and Lynch, L.N. (1998) Morphological study of coarse aggregates using image analysis. **Journal of Materials in Civil Engineering**, 10, 135-142.

Li, M.C., and Kett, I. (1967) Influence of coarse aggregate shape on the strength of asphalt concrete mixtures. **Highway Research Record 178**, 93-106.

Livneh, M. and Greenstein, J. (1972) Influence of aggregate shape on engineering properties of asphaltic paving mixtures. **Highway Research Record 404**, 42-56.

McLeod, N.W., and Davidson, J.K. (1981) Particle index evaluation of aggregates for asphalt paving mixtures. **Proceedings of Association of Asphalt Paving Technologists**, 50, 251-290.

Oduroh, P.K., Mahboub, K.C., and Anderson, R.M. (2000) Flat and elongated aggregates in Superpave regime. **Journal of Materials in Civil Engineering**, 12, 124-130.

Shklarsky, E. and Livneh, M. (1964) The use of gravels for bituminous mixtures. **Proceedings of Association of Asphalt Paving Technologists**, 33, 23-65.

Stephens, J.E., and Sinha, K.C. (1978) Influence of aggregate shape on bituminous mix character. **Journal of Association of Asphalt Paving Technologists**, 47, 434-456.

Yue, Z., Bekking, W., and Morin, I. (1995) Application of digital image processing to quantitative study of asphalt concrete microstructure. **Transportation Research Record 1492**, 53-60.

Zingg, T. (1935) Bietrahe zur schotteranalyse. **Schweiz Mineral Petrography**, 15, 39-140.